Journal of Hazardous Materials 199–200 (2012) 151–157

Contents lists available at SciVerse ScienceDirect

Journal of Hazardous Materials

journal homepage: www.elsevier.com/locate/jhazmat

Integration of processes induced air flotation and photo-Fenton for treatment of residual waters contaminated with xylene

Syllos S. da Silva[a], Osvaldo Chiavone-Filho[a,*], Eduardo L. de Barros Neto[a], Claudio A.O. Nascimento[b]

[a] Departamento Engenharia Química, NUPEG, Universidade Federal do Rio Grande do Norte, Campus Universitário, Lagoa Nova, Natal 59066-800, RN, Brazil
[b] Departamento de Engenharia Química, Escola Politécnica, Universidade de São Paulo, Cidade Universitária, São Paulo 05508-900, SP, Brazil

ARTICLE INFO

Article history:
Received 14 May 2011
Received in revised form
30 September 2011
Accepted 25 October 2011
Available online 29 October 2011

Keywords:
Xylene
Photo-Fenton
Flotation

ABSTRACT

Produced water in oil fields is one of the main sources of wastewater generated in the industry. It contains several organic compounds, such as benzene, toluene, ethyl benzene and xylene (BTEX), whose disposal is regulated by law. The aim of this study is to investigate a treatment of produced water integrating two processes, i.e., induced air flotation (IAF) and photo-Fenton. The experiments were conducted in a column flotation and annular lamp reactor for flotation and photodegradation steps, respectively. The first order kinetic constant of IAF for the wastewater studied was determined to be 0.1765 min^{-1} for the surfactant EO 7. Degradation efficiencies of organic loading were assessed using factorial planning. Statistical data analysis shows that H_2O_2 concentration is a determining factor in process efficiency. Degradations above 90% were reached in all cases after 90 min of reaction, attaining 100% mineralization in the optimized concentrations of Fenton reagents. Process integration was adequate with 100% organic load removal in 20 min. The results of the integration of the IAF with the photo-Fenton allowed to meet the effluent limits established by Brazilian legislation for disposal.

1. Introduction

Several wastewaters with environmental-polluting potential are generated along the entire productive oil chain [1–3]. In the explotation, the oil produced is usually mixed with water. This mixture depends upon the field maturity, and the water/oil ratio grows over time, and may reach up to 95% of well production [4]. The aqueous fraction removed from the well along with the oil is known as oil production water or produced water.

This wastewater is a hydrocarbon subproduct in underground reservoirs and generally contains high salinity, oil, various organic compounds such as benzene, toluene, ethylbenzene, xylene (BTEX), naphthalene, phenanthrene, dibenzothiophene (NFD), polyaromatic hydrocarbons (HPA), phenols, gases and heavy metals [5]. Therefore, the improper disposal of these wastewaters causes serious environmental damage, which is aggravated by the large volume involved, given the presence of these hydrocarbons in diluted concentrations.

Oil removal is one of the most important steps in treating this petroleum industry wastewater. Oil in produced water is present in four distinct forms, depending on its drop diameter, as follows: free, dispersed, emulsified and dissolved [6,7]. Oil distribution in these forms is a function of oil composition, pH, salinity, total dissolved solids, temperature, oil/water ratio, type and amount of oil field products [8]. In Brazil, resolution 393/07 of the National Environmental Council (CONAMA) establishes 29 ppm as the maximum disposal limit of total oil and grease (TOG) contained in the produced water [9].

Flotation is one of the most widely used separation processes for recovering oil present in the dispersed and emulsified phases of oily wastewater [10–12]. In this method, hydrophobic particles are selectively adsorbed on the gas bubble surface, normally air, and float to the surface where they are concentrated and removed along with the foam [13]. This unit operation is simple, highly efficient in contaminant removal, capable of medium and high flow rates, has low operation costs and short residence time, resulting in smaller spaces and construction economies [14].

The probability of a particle reaching the surface depends on the success of three stages: collision (P_C), adhesion (P_A) and transport (P_T) [15]:

$$P_F = P_C * P_A * P_T \quad (1)$$

The term collision refers to the probability of a collision between a particle and the air bubble. The probability of this stage is proportional to the ratio between particle and air bubble diameters.

$$P_C \alpha \left(\frac{D_P}{D_b}\right)^2 \quad (2)$$

* Corresponding author. Tel.: +55 84 3215 3773; fax: +55 84 215 3770.
E-mail address: osvaldo@eq.ufrn.br (O. Chiavone-Filho).

0304-3894/$ – see front matter © 2011 Elsevier B.V. All rights reserved.
doi:10.1016/j.jhazmat.2011.10.070

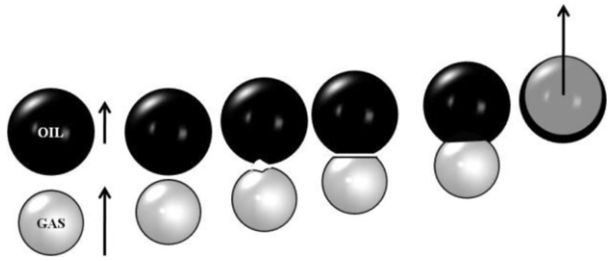

Fig. 1. Bubble–particle mechanism in induced-air flotation (IAF): collision, adhesion and bubble formation on the particle surface.

After the bubble–particle collision, a cluster should form. Surfactant agents act to reduce the contact angle formed during collision by decreasing interfacial tension [14], thereby favoring flotation (Fig. 1).

Eq. (2) shows that the smallest particles, that is, those that represent the dissolved fraction, are more difficult to be removed by flotation. The literature presents alternative techniques for removing the oil residual fraction [16–19]. Among these techniques, advanced oxidation processes (AOP), UV/H_2O_2, Fenton, photo-Fenton, UV/O_3 and UV/TiO_2 promote organic matter mineralization instead of phase transfer, normally found in physical processes [20–23].

The photo-Fenton can be divided into two stages with respect to hydroxyl radical formation (•OH). Initially, ferrous iron oxides are oxidized into ferric iron oxides in the presence of hydrogen peroxide (Eq. (3)), Fenton reaction [24]. In the next stage, ferric oxides generated in the Fenton reaction are photocatalytically converted to ferrous ions (Eq. (4)) [25].

$$Fe^{2+} + H_2O_2 \rightarrow Fe^{3+} + HO^{\bullet} + OH^{-} \quad (3)$$

$$[Fe(OH)]^{2+} \xrightarrow{h\nu} Fe^{2+} + HO^{\bullet} \quad (4)$$

In the presence of organic matter, the hydroxyl radical reacts with it, giving rise to oxidized products (Eq. (5)).

$$HO^{\bullet} + RH \xrightarrow{\text{chain propagation}} CO_2 + H_2O \quad (5)$$

A series of authors has pointed out process integration as being the most adequate solution for treating industrial wastewaters [26–28]. The aim of this study is to evaluate the efficiency of induced air flotation (IAF) and photo-Fenton integrated process in treating produced water to remove organic compounds.

2. Materials and methods

2.1. Materials

EO 7 is a commercial surfactant ethoxylated derived from fatty alcohol supplied by Oxiteno®. In order to characterize this surfactant, the following parameters have been determined, i.e., hydrophile–lipophile balance (HLB), critical micelle concentration (CMC) and thermal decomposition temperature (Table 1). The other used reagents have analytical grade, with minimum purity of 99%. They were supplied by VETEC with the following specifications: xylene (C_8H_{10}; mixture containing orto, meta and para-xylene), methanol (CH_3OH), ferrous sulfate heptahydrate ($FeSO_4 \cdot 7H_2O$) and hydrogen peroxide (H_2O_2; 30%, v/v).

Table 1
Physicochemical properties from EO 7.

Molar mass (g mol^{-1})	HLB	CMC (g L^{-1}) [29]	CMC (M)	Thermal decomposition temperature (°C)
494	12.5	0.0272	5.51 E−05	398

HLB, hydrophile–lipophile balance; CMC, critical micelle concentration.

Table 2
Thermodynamic properties of the BTEX group [30].

Compound	Water solubility 25 °C (ppm)	Normal (1 atm) boiling point (°C)	Vapor pressure at 20 °C (mmHg)
Ethylbenzene	161.5	136.1	4.53
Benzene	1785.5	80.0	95.20
m-Xylene	161.5	139.1	8.30
o-Xylene	171.5	144.5	6.60
p-Xylene	181.6	138.3	3.10
Toluene	532.6	110.6	28.4

Table 3
Complete experimental factorial design 2^2 from photodegradation of xylene.

x_i	−1	0	+1
[Fe^{2+}] mM	0.26	0.63	1
[H_2O_2] mM	40	95	150

2.2. Synthetic wastewater preparation

Synthetic wastewater was prepared from a mixture of xylene in distilled water. This organic compound was chosen as model to represent produced water oil field in term of organic loading. This was because of xylene relative high solubility in water and low vapor pressure compared to other hydrocarbons components (Table 2). Wastewater preparation was performed to ensure the presence of the aromatic hydrocarbons in the dispersed and dissolved aqueous phases, allowing the evaluation of the IAF and photo-Fenton stages, respectively.

For AIF tests, 10 mL of xylene in 2 L of distilled water and the system was maintained under agitation (22,500 rpm) for 2 h. To allow separation of excess xylene, the system was left resting for 2 h. Next, the surfactant was mixed to the wastewater and then added to the column.

Wastewater preparation was similar for the photodegradation experiments. A total of 10 mL of xylene was added to 1 L of distilled water and kept under agitation for 30 min. The system was left resting for 6 h. Excess xylene was used to promote two liquid phases after agitation and thus reach aqueous phase saturation with xylene.

3. Experimental procedure

3.1. Induced air flotation (IAF)

An air-induced aeration system with a constant flow rate of 700 cm^3 min^{-1} was used. The compressed air current passes through a porous plate filter (pore size varying from 16 to 40 μm) to promote the formation of small bubbles, estimated to be of 1 mm of diameter, followed by introduction into the wastewater. The dimensions of the flotation column measures are as follows: 0.93 m in height, 0.048 m of internal diameter, 0.050 m of external diameter and 1.5 cm^3 of volume. A foam collector and a trap to absorb the fraction dragged by the air flow were coupled to the column (Fig. 2).

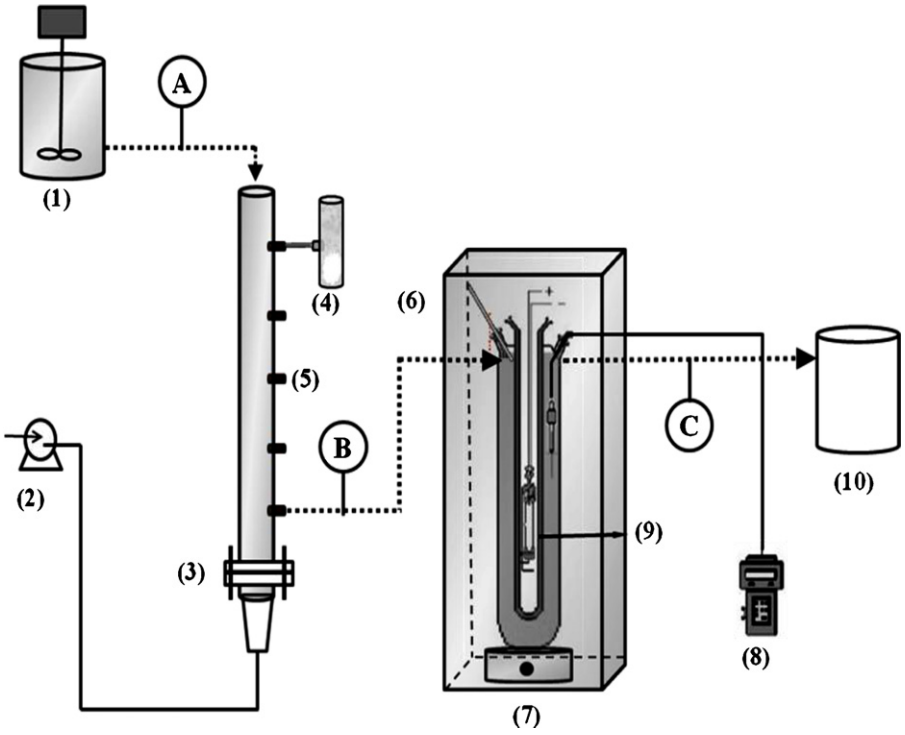

Fig. 2. Schematic diagram of the integrated column flotation process and photo-Fenton process in ascending flow annular lamp reactor to remove the TOG from oil field produced water; (1) mixing tank with raw wastewater; (2) compressed air; (3) porous plate; (4) foam sample collector; (5) sample collector; (6) sample collection and addition of hydrogen peroxide; (7) magnetic stirrer; (8) digital thermometer; (9) mercury vapor lamp; (10) treated wastewater; (A) sampling before flotation; (B) sampling after flotation; (C) sampling after photo-Fenton.

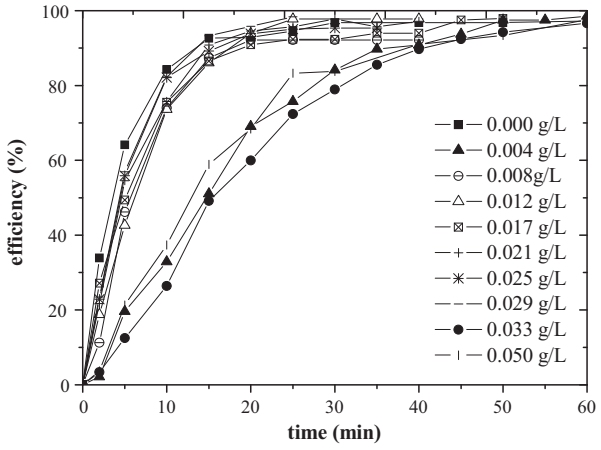

Fig. 3. Efficiency of xylene removal using EO 7 surfactants.

Xylene concentration in the samples was determined by UV–visible absorption molecular spectroscopy based on a calibration curve with a volume of 100 mL per sample gravimetrically prepared (in range to 0 at 600 ppm). The experimental uncertainty for the xylene determination by this UV spectroscopy procedure was determined to be 15 ppm. The dispersed aromatic hydrocarbon was solubilized in alcohol solution (30% by volume of CH_3OH) before analysis.

3.2. Photo-Fenton

It was used a 0.9 L ascending flow annular lamp reactor, properly sealed to avoid solute evaporative losses. A high-pressure 400 W mercury vapor lamp (from FLZ) was positioned inside a quartz well, on the longitudinal axis of the reactor. System temperature was measured with a thermometer placed inside of the wastewater. A scheme of the device is shown in Fig. 2.

Wastewater acidification up to a pH range between 2.5 and 3.0 was conducted within the reactor itself with a concentrated solution of H_2SO_4 [31]. $FeSO_4$ was then dissolved in the reaction medium. The reactor was operated semi-continuously with a dosage of hydrogen peroxide solution performed in three equal parts immediately after sample collections at 0, 20 and 45 min.

To study Fenton reagent concentrations in photodegradation, 2^2 factorial experimental planning was performed (Table 3). Kinetic determination of liquid-phase degradation was followed by TOC (total organic carbon) analysis. Vapor phase concentration was measured by gas chromatography [32].

4. Results and discussion

4.1. Flotation

Flotation kinetics was evaluated as a function of reduced xylene concentration in the wastewater (Eq. (6)). Fig. 3 shows the kinetics of xylene removal as a function of the concentration of the surfactant studied (EO 7).

$$E(\%) = \left(\frac{C_0 - C}{C_0}\right) \times 100 \quad (6)$$

where C_0 is the initial concentration of xylene and C is the concentration of xylene in time t.

Fig. 4 shows a high xylene removal rate for all the concentration of surfactant tested in the first 15 min, after which a tendency to stabilization occurs. Xylene removal rate as a function of time can be described by Eq. (7), under constant temperature, air flow,

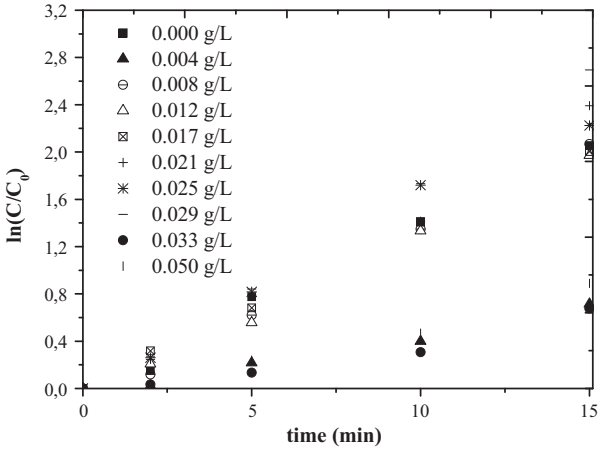

Fig. 4. Kinetics of xylene removal using EO 7 at various concentrations.

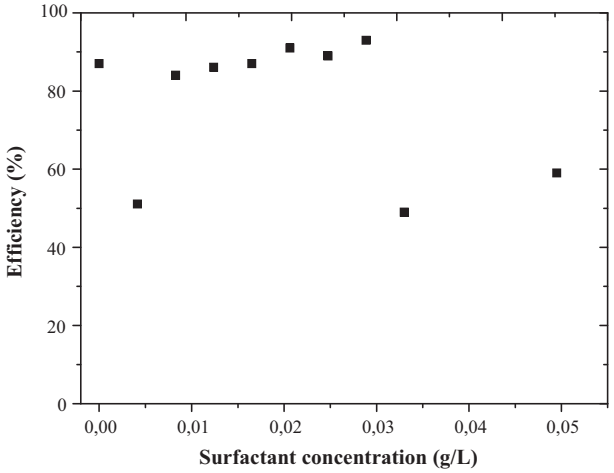

Fig. 5. Xylene removal as a function of EO 7 concentration.

Table 4
Velocity constants as a function of concentration used.

$C_{EO\ 7}$ (g L^{-1})	(R^2)[b]	k (min^{-1})
0.000	0.992	0.1388
0.004	0.975	0.0448
0.008	0.990	0.1193
0.012	0.995	0.1303
0.017	0.998	0.1361
0.021	0.993	0.1539
0.025	0.988	0.1559
0.029[a]	0.997	0.1765
0.033	0.932	0.0394
0.050	0.968	0.0545

[a] CMC.
[b] Correlation coefficient.

bubble diameter and column volume. The fit of the first order model to the data was adequate (Eq. (8)).

$$\frac{dC_{xylene}}{dt} = -k \cdot C_{xylene}^{n} \quad (7)$$

$$\ln\left(\frac{C_0}{C_t}\right) = k \cdot t \quad (8)$$

where C_{xylene} = concentration of xylene (g L^{-1}), C_0 = initial concentration of xylene (g L^{-1}), C_t = concentration of xylene in time t (g L^{-1}), k = kinetic constant (min^{-1}), t = flotation time (min), n = order of kinetics of the removal process.

The first-order kinetic model is based on the presumption that the bubble–particle collision rate is first order in relation to the number of particles and that bubble concentration remains constant over time [33]. Constant k in Eq. (7) encompasses aeration, reagent concentration, particle size, previous treatment and type of flotation cell.

Other studies showed first-order kinetics in industrial wastewater treatment [33–35]. Fig. 4 shows linear regression results for the first 15 min of flotation using EO 7 surfactant.

Table 4 shows that an increase in surfactant concentration leads to an increase in kinetic constant up to a maximum concentration and, beyond this optimal value, it falls. The increased surfactant concentration covers the xylene drop, enabling coalescence and increasing k value until maximum efficiency is reached. This can be easily seen in values below CMC [11].

Fig. 5 shows the separation efficiency of EO 7 as a function of surfactant concentration for 15 min of flotation. Efficiency grows until it reaches CMC.

When surfactant in the mixture is below its CMC, it adsorbs on the surface of the xylene drop, partially covering it, enabling system coalescence, and consequently resulting in better contact and the surfactant being dragged by the air bubbles to the top of the column. Because surfactant concentration is above CMC, surfactant monomers adsorbed on the xylene–water surface completely cover it, avoiding coalescence of xylene drops.

It was observed an elevated removal of xylene without the presence of surfactant, which is supported by the striping gas effect. During the flotation, xylene is transferred to the gas phase due to the release of bubbles at the surface, dragging the contaminant in a simultaneous form, i.e., flotation and striping [36]. In the cases where there are only non volatile organic compounds, as contaminants, the removal efficiency reaches about 80 and 50% with and without surfactant, respectively [11].

4.2. Photo-Fenton

Preliminary experiments were conducted to assess the occurrence of xylene evaporative losses during the experiments (Fig. 6). The blank assay, without the addition of Fenton reagents, showed practically constant xylene concentration over time. In the preliminary photodegradation experiment, liquid and vapor phases demonstrated that no evaporation mass transfer occurred, but rather degradation. Xylene concentrations in aqueous and vapor phases were determined by total organic carbon analyses and

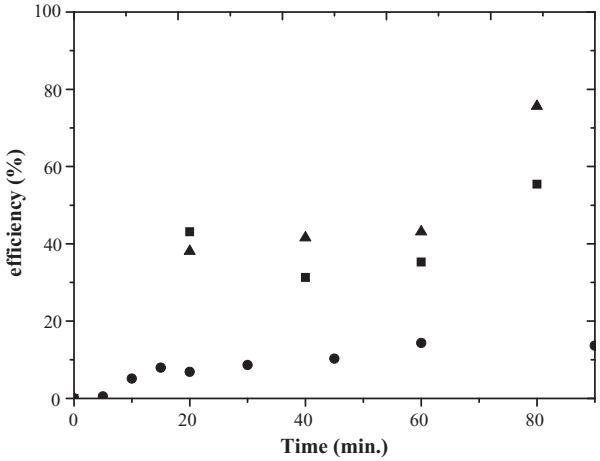

Fig. 6. Preliminary xylene photodegradation experiments (300 mM H_2O_2 and 1 mM Fe^{2+}): (●) without adding Fenton reagents; (▲) liquid phase; (■) vapor phase in a closed system.

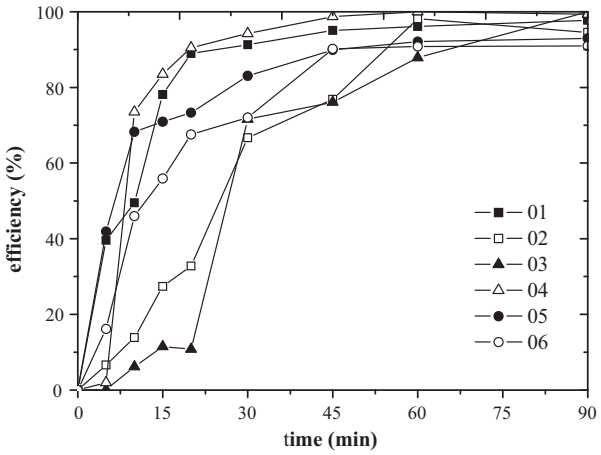

Fig. 7. Degradation of xylene in aqueous: 01 (150 mM H_2O_2 and 0.26 mM Fe^{2+}), 02 (40 mM H_2O_2 and 0.26 mM Fe^{2+}), 03 (40 mM H_2O_2 and 1 mM Fe^{2+}), 04 (150 mM H_2O_2 and 1 mM Fe^{2+}), 05 (95 mM H_2O_2 and 0.63 mM Fe^{2+}) and 06 (95 mM H_2O_2 and 0.63 mM Fe^{2+}).

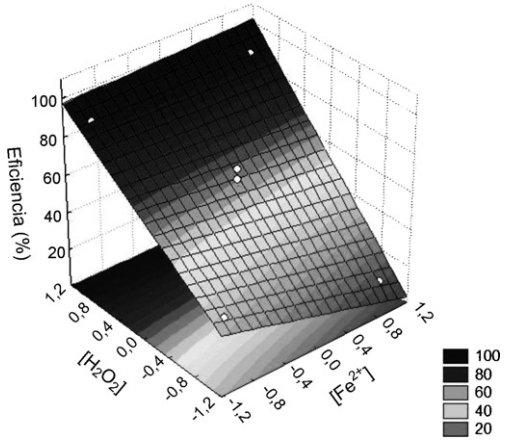

Fig. 8. Response surface of complete 2^2 factorial planning for efficient xylene removal by photo-Fenton process as a function of hydrogen peroxide and ferrous sulfate inputs.

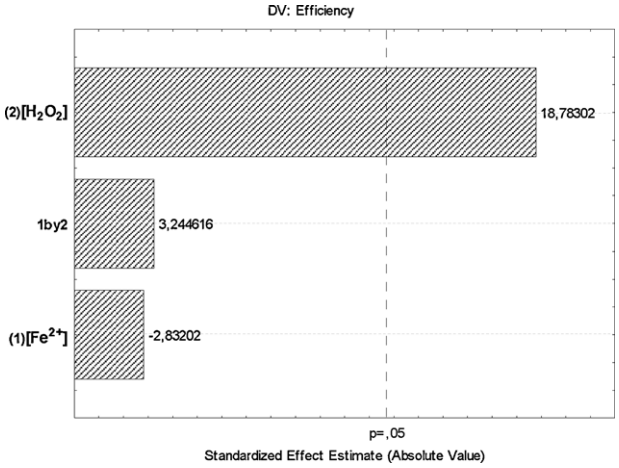

Fig. 9. Pareto graph for xylene removal by photo-Fenton process as a function of hydrogen peroxide and ferrous sulfate inputs.

chromatography, respectively (Fig. 6). It was therefore possible to confirm that no significant solute loss occurred by evaporation or any other undesirable mechanism.

Fig. 7 depicts xylene degradation using the photo-Fenton process in an annular reactor with a 400 W lamp. For the Fenton reagent concentrations established by experimental planning, final efficiencies were very similar, ranging from 90% to total organic load mineralization (100%). However, a significant difference in degradation efficiency occurred at 20 min of reaction.

After 20 min of reaction, 90.5% removal of xylene is reached using 1 mM de Fe^{2+} and 150 mM H_2O_2 (Fig. 7 – curve 4). However, a slightly lower efficiency (89%) is obtained for the same reaction time using 0.26 mM de Fe^{2+} and 150 mM H_2O_2 (Fig. 7 – curve 1). From the economic and environmental standpoints, this is the best option considering that the Brazilian limit for iron disposal is 0.27 mM. Operating under this latter condition, wastewater meets the established regulation, thereby avoiding additional metal removal costs. Using the minimum concentration of Fenton reagents, the efficiency achieved at the end of the test was 94.5%. However, to reach this percentage, a reaction is three times longer than that found in curve 1 conditions is required (Fig. 7). This is essential because the longer the reaction time, the larger the area needed, which increases investments and indirect costs as well as the volume/capacity of equipment used in produced water treatment plants. Slower degradation occurred when concentrations of 40 mM H_2O_2 and 1 mM Fe^{2+} were used.

The response surface for experimental data obtained shows that the highest degradation occurs with maximum peroxide concentration (Fig. 8). With respect to ferrous ions, efficiency values were very similar for the Fe^{2+} concentration range studied (Fig. 8). However, owing to previously mentioned environmental and economic factors, it is recommended that the minimum value of iron and maximum of peroxide be used.

The Pareto graph (Fig. 9) shows that the most influential variable in this process is peroxide concentration. The mathematical model for photodegradation efficiency (η) is illustrated in Eq. (9), where x_1 is the ferrous sulfate normalized concentration and x_2 peroxide hydrogen normalized concentration.

$$\eta(\%) = 58.83 - 5.12x_1 + 33.97x_2 + 5.86x_1x_2 \quad (9)$$

4.3. IAF and integrated photo-Fenton processes

The efficiency of integrated IAF and photo-Fenton processes in organic load removal of synthetic oil field wastewater is shown in Fig. 10. In both cases, the best conditions previously observed for surfactant and Fenton reagent concentrations with xylene were considered.

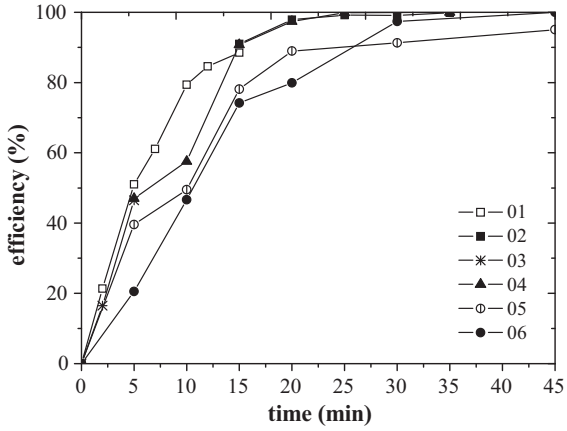

Fig. 10. Removal of organic matter using the flotation (curves 1, 3) and photo-Fenton process (curves 2, 4, 5, 6) of synthetic produced water with xylene.

Fig. 10 depicts efficiency removal curves for the series of experiments performed. The wastewater remained in the flotation experiments (curves 1 and 3) was then submitted to the

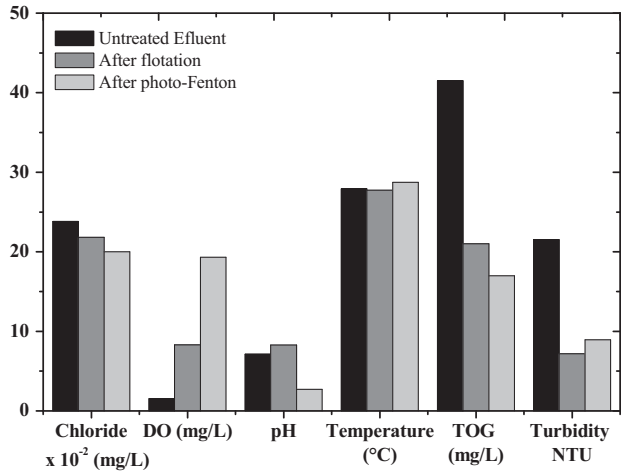

Fig. 11. Assessment of physicochemical parameters of integrated flotation and photo-Fenton processes to remove TOG from produced water in oil fields.

photodegradation process in lamp reactor (curves 2 and 4) to remove the organic load remaining from the first stage of flotation. One wastewater containing xylene at saturation, i.e., maximum dissolved concentration, was directly submitted to the photo-Fenton process without AIF pretreatment (curve 5). Another wastewater, prepared using dispersed xylene, i.e., with concentration over to the saturation, was also submitted to the photo-Fenton process without IAF pretreatment (curve 6). After 15 min (curve 1) and 5 min (curve 3) of pretreatment in flotation column resulted in removal of xylene of 90% and 20% of TOC, respectively. In the first condition resulted more efficient, demanding a reaction time in the photodegradation stage of just 5 min to reach complete mineralization. In the second case, the reaction time needed for mineralization was 4 times greater. Curves 5 and 6 show that the kinetics of the photo-Fenton process becomes slower when it is not preceded by IAF. When xylene concentration is above its saturation limit (curve 6), the photo-oxidation process depends upon the dissolution of the solute, resulting a slower process.

As the experiments were performed in a semi-continuous process, it should be underscored that a single dosage of hydrogen peroxide was needed for 15 min of flotation, while for the other conditions two dosages were required to reach complete mineralization, thereby increasing reagent costs.

Therefore, the results obtained indicate that the best option is integrating IAF and photo-Fenton processes for treating the wastewater under study.

4.4. Integrated IAF and photo-Fenton processes applied to the real oil field produced water

The results of experiments conducted with real produced water from the state of Rio Grande do Norte, Brazil were also satisfactory (Fig. 11). The real sample of produced water from oil field was submitted to 15 min of flotation resulted in a 49% and 67% decrease in TOG and turbidity respectively and, as expected, a significant increase in dissolved oxygen (DO) concentration (Fig. 11). The reductions in TOG and turbidity levels are due to removal of the oil fraction present in the dispersed phase.

Next, the clarified wastewater remained was submitted in the lamp reactor for 15 min. At the end of integration, a reduction of 59% and 58% of TOG and turbidity respectively was achieved. Dissolved oxygen concentration increased by more than 10-folders when compared to the original value. The reduction in pH was due to wastewater acidification between 2.5 and 3.0, the range required for the photo-Fenton process [37]. The total removal in terms o TOG was 59%.

5. Conclusions

Experimental data obtained from column flotation showed first order kinetic behavior. For surfactant concentrations below CMC, separation efficiency increases with an increase in surfactant concentration. For the concentrations studied, the best condition found was 0.029 g L^{-1} for EO 7 with velocity constant of 0.1765 min^{-1}. A removal efficiency of 98% was obtained after 30 min.

As with flotation, the photo-Fenton process proved to be efficient in removing xylene. The advantage of this process over the previous method is pollutant elimination instead of phase transference.

Organic load degradation efficiency was 90.5% and 89% using 1 mM of Fe^{2+} and 150 mM H_2O_2 and 0.26 mM of Fe^{2+} and 150 mM H_2O_2, respectively, after 20 min of the photo-Fenton experiment. From the economic and environmental standpoint, the best condition uses the lowest Fe^{2+}concentration. For all concentrations in the photo-Fenton process, organic load mineralization (100%) can be attained at the end of the experiment (90 min).

For the synthetic wastewater, integration was the best option for 100% removal of the entire organic load in 20 min, 15 min of IAF and 5 min of photo-Fenton.

The results obtained with real wastewater classified it within the allowable legal limits for the parameters analyzed. Oil recovered in the flotation stage can be redirected to the oil treatment stage for refining purposes, without causing distillation problems, given that the degradation temperature of the surfactant is lower than the operation temperature of distillation columns.

Acknowledgments

Brazilian financial support provided by ANP (Agência Nacional do Petróleo), CAPES (Coordenação de Aperfeiçoamento de Pessoal de Nível Superior), CNPq (Conselho Nacional de Desenvolvimento Científico e Tecnológico) and INCT-EMA (Institutos Nacionais de Ciência e Tecnologia de Estudos do Meio Ambiente) are gratefully acknowledged.

References

[1] M.A.G. Pivel, C.M.D.S. Freitas, J.L.D. Comba, Modeling the discharge of cutting sand drilling fluids in a deep-water environment, Deep-Sea Res. II 56 (2009) 12–21.
[2] M.J. Ayotamuno, R.N. Okparanma, S.O.T. Ogaji, S.D. Probert, Chromium removal from flocculation effluent of liquid-phase oil-based drill-cuttings using powdered activated carbon, Appl. Energy 84 (2007) 1002–1011.
[3] L. Yana, H. Ma, B. Wang, W. Mao, Y. Chena, Advanced purification of petroleum refinery wastewater by catalytic vacuum distillation, J. Hazard. Mater. 178 (2010) 1120–1124.
[4] D.F. Boesch, N.N. Rabalais, Long-term Effects of Offshore Oil and Gas Development, Taylor and Francis, London, 1987.
[5] J.M. Neff, Bioaccumulation in Marine Organisms Effect of Contaminants From Oil Well Produced Water, Elsevier, Amsterdam, 2002.
[6] M. Cheryan, N. Rajagopalan, Membrane processing of oily streams, wastewater treatment and waste reduction, J. Membr. Sci. 151 (1998) 13–18.
[7] J.A. Veil, M.G. Puder, D. Elcock, R.J. Redweik Jr., A White Paper Describing Produced Water From Production of Crude Oil, Natural Gas, and Coal Bed Methane, Argonne National Laboratory, Pittsburgh, 2004.
[8] F.R. Ahmadum, A. Pendashteh, L.C. Abdullah, D.R.A. Biak, S.S. Madaeni, Z.Z. Abidin, Review of technologies for oil and gas produced water treatment, J. Hazard. Mater. 170 (2009) 530–551.
[9] Conselho Nacional do Meio Ambiente – CONAMA, Resolução n° 393, de 8 de agosto de 2007.
[10] K. Bensadok, M. Belkacem, G. Nezzal, Treatment of cutting oil/water emulsion by coupling coagulation and dissolved air flotation, Desalination 206 (2007) 440–448.
[11] L.M.O. Lima, J.H. Silva, A.A.R. Patricio, E.L. Barros Neto, A.A. Dantas Neto, T.N.C. Dantas, M.C.P.A. Moura, Oily wastewater treatment through a separation process using bubbles without froth formation, J. Pet. Sci. Eng. 26 (2008) 994–1004.

[12] L. Xiao-Bing, L. Jiong-Tian, W. Yong-Tian, W. Cun-Ying, Z. Xiao-Hua, Separation of oil from wastewater by column flotation, J. China Univ. Mining Technol. 17 (2002) 546–551.
[13] A.V. Nguyen, H.J. Schulze, Colloidal Science of Flotation, Marcel Dekker, New York, 2004.
[14] J. Rubio, M.L. Souza, R.W. Smith, Overview of flotation as a wastewater treatment technique, Miner. Eng. 15 (2002) 139–155.
[15] R.H. Yoon, The role of hydrodynamic and surface forces in bubble–particle interaction, Int. J. Miner. Process. 58 (2000) 129–143.
[16] Z. Cha, C. Lin, C. Cheng, P.K. Hong, Removal of oil and oil sheen from produced water by pressure-assisted ozonation and sand filtration, Chemosphere 78 (2010) 583–590.
[17] G.T. Tellez, N. Nirmalakhandan, J. Gardea-Torresdey, Performance evaluation of an activated sludge system for removing petroleum hydrocarbons from oilfield produced water, Adv. Environ. Res. 6 (2002) 455–470.
[18] C.R. Altare, R.S. Bowman, L.E. Katz, K.A. Kinney, E.J. Sullivan, Regeneration and long-term stability of surfactant-modified zeolite for removal of volatile organic compounds from produced water, Micropor. Mesopor. Mater. 105 (2007) 305–316.
[19] J.E.F. Moraes, F.H. Quina, D.N. Silva, O. Chiavone-Filho, C.A.O. Nascimento, Utilization of solar energy in the photodegradation of gasoline in water and of oilfield-produced water, Environ. Sci. Technol. 38 (2004) 3746–3751.
[20] T. Garoma, M.D. Gurol, O. Osibodu, L. Thotakura, Treatment of groundwater contaminated with gasoline components by an ozone/UV process, Chemosphere 73 (2008) 825–831.
[21] S. Papiïc, D. Vujevi ïC, N. Koprivanac, D. Sinko, Decolourization and mineralization of commercial reactive dyes by using homogeneous and heterogeneous Fenton and UV/Fenton processes, J. Hazard. Mater. 164 (2009) 1137–1145.
[22] M.S. Lucas, J.A. Peres, Removal of COD from olive mill wastewater by Fenton's reagent: kinetic study, J. Hazard. Mater. 168 (2009) 1253–1259.
[23] Q. Hu, C. Zhang, Z. Wang, Y. Chen, K. Mao, X. Zhang, Y. Xiong, M. Zhu, Photodegradation of methyl tert-butyl ether (MTBE) by UV/H_2O_2 and UV/TiO_2, J. Hazard. Mater. 154 (2008) 795–803.
[24] J.J. Pignatello, Dark and photoassisted Fe^{3+} – catalyzed degradation of chlorophenoxy herbicides by hydrogen peroxide, Environ. Sci. Technol. 26 (1992) 944–951.
[25] A. Safarzadeh-Amiri, J.R. Bolton, S.R. Cater, Ferrioxalate-mediated photodegradation of organic pollutants in contaminated water, Water Res. 31 (1997) 787–798.
[26] R.F. Sena, J.L. Tambosi, K. Genena, R.F.P.M. Moreira, H.F. Schröder, H.J. José, Treatment of meat industry wastewater using dissolved air flotation and advanced oxidation processes monitored by GC–MS and LC–MS, Chem. Eng. J. 152 (2009) 151–157.
[27] X.J. Wang, Y. Song, J.S. Mai, Combined Fenton oxidation and aerobic biological processes for treating a surfactant wastewater containing abundant sulfate, J. Hazard. Mater. 160 (2008) 344–348.
[28] M.M.B. Martin, J.A.S. Perez, F.G.A. Fernandez, J.L.C. Lopez, A.M. Garcia-Ripoll, A. Arque, I. Oller, S.M. Rodriguez, Combined photo-Fenton and biological oxidation for pesticide degradation: effect of photo-treated intermediates on biodegradation kinetics, Chemosphere 70 (2008) 1476–1483.
[29] M.J. Schick, Nonionic Surfactant Physical Chemistry, Marcel Dekker, New York, 1966.
[30] M. Farhadian, D. Duchez, C. Vachelard, C. Larroche, Monoaromatics removal from polluted water through bioreactors. A review, Water Res. 42 (2008) 1325–1341.
[31] R.F.P. Nogueira, A.G. Trovó, M.R. Silva, R.D. Villa, Fundamentos e aplicações ambientais dos processos Fenton e foto-Fenton, Quím. Nova 30 (2007) 400–408.
[32] Z.S.M.S. Evangelista, Thesis, Universidade Federal do Rio Grande do Norte, Natal, RN, 2009.
[33] M. Polat, S. Chander, First-order flotation kinetics models and methods for estimation of the true distribution of flotation rate constants, Int. J. Miner. Process. 58 (2000) 145–166.
[34] L.B. Mansour, S. Chalbi, Removal of oil from oil/water emulsions using electroflotation process, J. Appl. Electrochem. 36 (2006) 577–581.
[35] B. Ramaswamy, D.D. Kar, S. De, A study on recovery of oil from sludge containing oil using froth flotation, J. Environ. Manage. 85 (2007) 150–154.
[36] W.J. Parker, H.D. Monteith, Stripping of VOC's from dissolved air flotation, Environ. Prog. 15 (2) (1996) 73-81.
[37] J.J. Pignatello, E. Oliveros, A. Mackay, Advanced oxidation processes for organic contaminant destruction based on the Fenton reaction and related chemistry. Critical reviews, Environ. Sci. Technol. 36 (2006) 1–84.